ORIGINAL ARTICLE

Role of heterojunction $ZrTiO_4$/$ZrTi_2O_6$/TiO_2 photocatalyst towards the degradation of paraquat dichloride and optimization study by Box–Behnken design

Nur Afiqah Badli [1], **Rusmidah Ali** *, **Wan Azelee Wan Abu Bakar** [2], **Leny Yuliati** [3]

Department of Chemistry, Faculty of Science, Universiti Teknologi Malaysia, 81310 UTM, Johor Bahru, Johor, Malaysia

Abstract   This study revealed that the existence of heterojunction of $ZrTiO_4$/$ZrTi_2O_6$/TiO_2 in the photocatalyst system has significantly enhanced the photodegradation of paraquat dichloride with respect to the increment of it thermal stability as shown in the XRD and XPS analyses. Several parameters such as ZrO_2/TiO_2 ratios (10:90, 20:80 and 30:70) and catalyst dosage (0.1–0.4 g) have been studied to achieve the optimum degradation of paraquat dichloride. The kinetic study was determined by using various ZrO_2/TiO_2 ratios calcined at 750 °C and showed that the photodegradation of paraquat over ZrO_2/TiO_2 photocatalyst follows a pseudo first-order kinetic. The optimum condition was obtained using ZrO_2/TiO_2 (20:80), calcined at 750 °C and with 0.3 g catalyst dosage which gave 84.41% degradation after 240 min under UV irradiation, λ_{UV} = 365 nm. The N_2 adsorption–desorption analysis shows the mixture of Type III and IV isotherms with hysteresis loop type H2(b). Meanwhile, the Box–Behnken design showed the optimum photodegradation of paraquat was obtained at the calcination temperature of 750 °C, with the ZrO_2/TiO_2 ratio of 20:80 and 0.3 g catalyst dosage which was 0.24% lower than our experimental verification result.

* Corresponding author. Tel.: +60 197114144.
   E-mail addresses: nurafiqahbadli@gmail.com (N.A. Badli), rusmidah@kimia.fs.utm.my (R. Ali), wazelee@kimia.fs.utm.my (W.A. Wan Abu Bakar), leny@ibnusina.utm.my (L. Yuliati).
   [1] Tel.: +60 1371483768.
   [2] Tel.: +60 137466213.
   [3] Tel.: +60 197454870.
Peer review under responsibility of King Saud University.

Production and hosting by Elsevier

1. Introduction

An agricultural pesticide which contains hazardous organic compounds has led to the main environmental problem due to toxic properties and non-biodegradable properties of the compound in water. Paraquat dichloride (1,1-dimethyl-4,4′-bipyridylium dichloride) is common herbicide that was widely used in developed country due to the great feature such as high solubility in water and high binding potential. However, it may cause severe health problems to human such as Parkinson's disease and dysfunction of kidney (Dhaouadi

and Adhoum, 2009; Sorolla et al., 2012). Therefore, the degradation or removal of paraquat dichloride from water has become matter of paramount important.

Advanced oxidation processes (AOPs) employing heterogeneous catalysts have been used extensively for various types of degradation of organic pollutants in water. This is due to the ability of the catalyst to generate a strongly oxidizing hydroxyl radical with high oxidative power of $E_o = 2.8$ eV and thus acts to degrade various organic pollutants. Among the semiconductor photocatalyst used, titania (TiO_2) has been promoted as a potential photocatalyst that can be used for the degradation of the paraquat dichloride due to the ability to completely oxidize a large number of hazardous organic pollutants to non-toxic products (Madani et al., 2015; Santos et al., 2011).

According to the previous research, degradation of paraquat using commercial TiO_2 has shown only 17% of paraquat degradation after 4 h under UV irradiation (Lee et al., 2002). Nevertheless, doping or coupling of TiO_2 with other metal oxides shows synergic effect and had increased the percentage degradation of the organic pollutant. This might be due to the increase of the thermal stability and surface area as well as lowering the recombination rate of electron and hole in TiO_2 (Kim et al., 2008). Sorolla et al.(2012), have been reported that only 55% paraquat degradation was achieved using 2 wt.% Cu–TiO_2/SBA-15 after 4 h irradiation. Meanwhile, no paraquat degradation was observed using $Ti_{1-x}Fe_xO_2$ (Florêncio et al., 2004). Incorporation of zirconia with TiO_2 either as binary oxide or as solid solution photocatalyst had proven to have better photocatalytic activity for degradation of organic pollutant in the aqueous phase (Kim et al., 2012; Schiller et al., 2010).

In this study, the heterojunction of $ZrTiO_4$/$ZrTi_2O_6$/TiO_2 photocatalyst was successfully prepared using modified sol gel method and the photocatalytic activity was tested on the degradation of paraquat dichloride under UV irradiation for 240 min. Various ZrO_2/TiO_2 ratios and catalyst dosages have been studied to observe the effect on phase transformation of TiO_2 and surface area of the prepared photocatalyst. Interestingly, the formation of heterojunction of $ZrTiO_4$/$ZrTi_2O_6$/TiO_2 photocatalyst and rutile phase of TiO_2 at ratio anatase to rutile of 82:18 in the photocatalyst system has given positive effect on the degradation of paraquat dichloride. This is the new finding based on our best knowledge. Various analytical techniques were employed to reveal their physicochemical properties. The response surface analysis was used for optimization study and Box–Behnken design was applied to determine the optimum photodegradation of paraquat and also to explain the interaction among the parameters studied.

2. Experimental

2.1. Synthesis of Zr/Ti photocatalyst

TiO_2 was synthesized using titanium isopropoxide (TTIP) obtained from Sigma Aldrich as precursor via modified sol gel method. Firstly, 1.76 g of PEG 2000 (Merck) was dissolved in 70 mL of ethanol (QRec). Next, 6.15 g of diethanolamine (Merck) was added to the solution followed by 12.00 g of TTIP. Subsequently, 1.60 mL of distilled water was added slowly and stirred continuously for another 2 h at room temperature (Ali and Hassan, 2008). Zirconium (IV) oxynitrate hydrate that has been dissolved in 10 mL of distilled water was then added into the clear solution. The mixture was stirred for 2 h to get homogenous photocatalyst. Then, it was aged at room temperature for 2 days and dried at 100 °C for 24 h before calcined at 750 °C for 5 h. Lastly, the sample was grinded to fine powder. The ratios were varied based on weight percentage from 10:90, 20:80 and 30:70.

2.2. Photocatalytic activity measurement

The photocatalytic degradation was conducted in a Pyrex beaker and was placed inside a box with 365 nm UV irradiation source (100 V, 6 W). Then, 0.1 g of Zr/Ti photocatalyst was added into 250 mL 15 ppm of paraquat dichloride solution. The suspension was stirred in the dark for the adsorption of paraquat dichloride for 30 min before irradiated for 240 min. The sample was collected every 60 min for 240 min irradiation. UV–Vis spectrophotometer Model UV-2501Pc Shimadzu was used to measure the samples. The percentage of photocatalytic activity was calculated using Eq. (1),

$$\% \ D = \frac{A_o - A_t}{A_o} \times 100 \tag{1}$$

where % D is the percentage of degradation, A_o is the initial absorbance of sample before irradiation under UV light and A_t is the absorbance of sample after irradiation under UV-light (t-minutes). The experiment was repeated without the catalyst presence for photolysis reaction.

2.3. Characterization of the catalysts

X-ray diffraction analysis was done using Siemen D5000 diffractometer utilizing Cu Kα radiation ($\lambda = 1.54060$ Å). Data were collected in range of 2θ from 10° to 80° and analysed by software called Diffract Plus. XPS surface study was performed using Kratos surface analysis spectrometer XSAM HS instrument with Mg Kα (1253.6 eV) as the X-ray source. Transmission electron microscopy (TEM) was performed using JEOL-JEM 2100 operated at 200 kV. N_2 adsorption/desorption isotherm analysis was attained using Micromeritics ASAP 2010 volumetric adsorption analyser at -196 °C. Prior to the measurement, the calcined catalysts were degassed at 120 °C for 5 h. The DR UV–Vis spectra were measured by UV–vis spectroscopy model Perkin Elmer Lambda 550.

2.4. Response Surface Methodology (RSM)

The Response Surface Methodology (RSM) was used to validate the predicted value of the optimization parameter from RSM with actual value obtained from experiment. Design-Expert Version 7.1.6 software was used for generating and evaluating the statistical experimental design. To assess the interaction between parameters towards the degradation of paraquat dichloride (Y), three parameters were selected: calcination temperature (°C), ZrO_2/TiO_2 ratio and catalyst dosage (g). Total of 17 experiments were designed and performed in random order and levels of independent variables are displayed in Table 1.

3. Results and discussion

In this study zirconium was added to TiO_2 photocatalyst for in-depth investigation towards the effect of ZrO_2/TiO_2 ratios on the formation of ternary species which are $ZrTiO_4$ and $ZrTi_2O_6$ in the photocatalyst system towards the degradation of paraquat dichloride. The experiment was run for 240 min under UV irradiation. Our previous study had reported that calcination temperatures of 450 > 750 > 1000 °C for TiO_2

Table 1 The experiment values and level of independent variables.

Independent variable	Factor	Coded value		
		−1	0	1
Calcination temperature (°C)	A	700	750	800
ZrO₂/TiO₂ ratio	B	10	20	30
Catalyst dosage (g)	C	0.2	0.3	0.4

Table 2 Percentage of anatase phase and rutile phase at various ZrO₂/TiO₂ ratios calcined at 750 °C for 5 h.

Samples	Anatase (%)	Rutile (%)
(10:90)	57	43
(20:80)	82	18
(30:70)	100	–

and $750 > 450 > 1000\ °C$ for ZrO₂/TiO₂ (10:90) were observed which indicated that addition of zirconium at certain ratio had remarkable improvement over degradation of paraquat dichloride compared to the single TiO₂. The best calcination temperature for TiO₂ was 450 °C. Meanwhile for the ZrO₂/TiO₂ photocatalyst it was 750 °C at ZrO₂/TiO₂ ratio of 20:80 (Badli et al., 2015). In this paper, the ZrO₂/TiO₂ photocatalyst was further optimized at various ZrO₂/TiO₂ atomic ratios and catalyst dosage to investigate the formation of ternary species thus increasing the photodegradation activity.

3.1. Characterization of catalyst

Fig. 1 shows the diffractograms of XRD analysis for ZrO₂/TiO₂ photocatalyst at various ZrO₂/TiO₂ ratios. The XRD analysis showed the tetrahedral structure of anatase TiO₂ was displayed at diffraction peaks of $2\theta = 25.3°$ (I_{99}), 48.0° (I_{24}), 37.6° (I_{18}), 53.9° (I_{15}) and 55.1 (I_{15}) in all samples. The percentage of anatase and rutile phases was calculated according to Eq. (2) and is tabulated in Table 2.

$$A\% = \frac{I_A}{I_A + 1.256 I_R} \times 100 \tag{2}$$

where A is the anatase content, I_A is the intensity of anatase and I_R is the intensity of rutile.

The presence of Zr as shown in Fig. 1(a) has delayed the phase transformation of TiO₂ at high temperature which was also reported by Kim et al. (2012). In addition, the new ternary species belong to orthorhombic structure of ZrTi₂O₆ (JCPDS 00-046-1265) at 2θ value of 30.71° (I_{100}) and second highest peak at 24.87° (I_{72}) was observed, while for ZrTiO₄ (JCPDS 00-007-0290) occurred at value 30.59° (I_{100}) and second highest peak at 24.71° (I_{16}) were also observed at ZrO₂/TiO₂ ratio of 20:80 and 30:70. Besides that, no diffraction peak due to ZrO₂ could be detected in all samples suggesting that the ZrO₂ might be formed in the bulk matrix of TiO₂ or was well dispersed in the catalyst surface and cannot be detected using XRD analysis.

The anatase diffraction peak (1 0 1) was slightly shifted to lower angle suggested that the Zr was merged in the lattice of TiO₂ as shown in Fig. 1(b) and affects the lattice parameter and d-spacing value for ZrO₂/TiO₂ photocatalyst as tabulated in Table 3. The enhancement of distance between the crystal planes was due to the substitution of Zr ion which has larger ionic radius (0.072 nm) compared to Ti ion (0.065 nm) as has also been reported by Kim et al. (2008) and Venkatachalam et al. (2007).

XPS analysis was conducted to measure the chemical composition and electronic state of ZrO₂/TiO₂ (20:80) calcined at 750 °C which showed the best photodegradation of paraquat dichloride. Fig. 2 shows the XPS spectra of Ti 2p, Zr 3d and O 1s that has been deconvoluted into components. From the Ti $2p_{3/2}$ three peaks of Ti⁴⁺ (457.21, 458.31 and 459.45 eV) were obtained belonging to ZrTi₂O₆, TiO₂ and ZrTiO₄ respectively (NIST XPS database). Meanwhile for the Zr $3d_{5/2}$ spectra, there are two peaks for Zr⁴⁺ (181.54 and 182.01 eV) which can be assigned to the ZrTi₂O₆ and ZrTiO₄ respectively and also obtained by Gnatyuk et al. (2010).
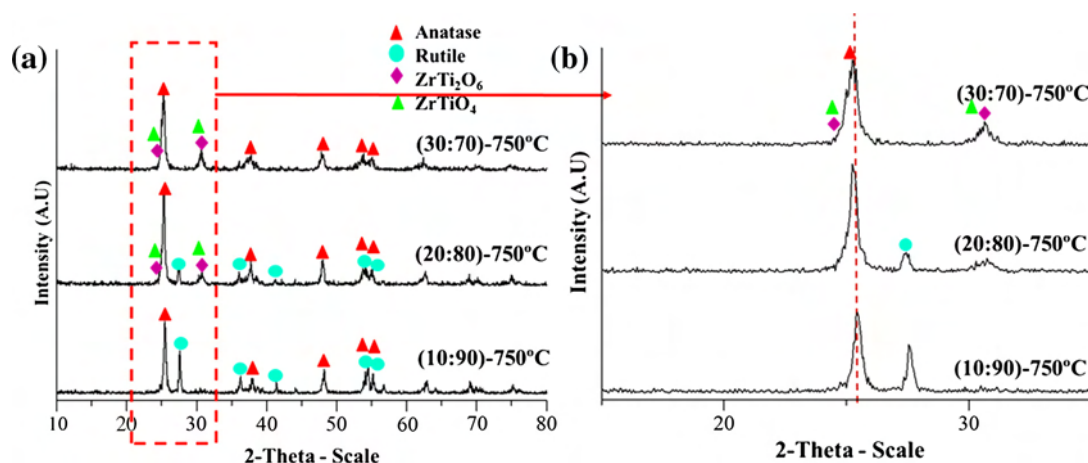

Figure 1 XRD diffractogram patterns of (a) ZrO₂/TiO₂ photocatalyst and (b) zoom-in XRD diffractogram patterns of the anatase (1 0 1) diffraction peaks at various ZrO₂/TiO₂ ratios and were calcined at 750 °C for 5 h. The PDF referenced of Ti₂ZrO₆ (JCPDS 00-046-1265) and TiZrO₄ (JCPDS 00-007-0290).

Table 3 Properties of ZrO₂/TiO₂ photocatalyst at various ZrO₂/TiO₂ ratios calcined at 750 °C for 5 h.

Samples	$d_{(101)}$ value[a] (Å)	Lattice parameter, a[b]	Surface area[c] (m²/g)	Average pore diameter[d] (Å)	Band gap[e] (eV)
(10:90)	3.4951	4.9428	41.58	170.45	3.05
(20:80)	3.5172	4.9741	46.35	177.21	3.06
(30:70)	3.5195	4.9773	34.32	163.89	3.16

[a] The value was calculated from $2d_{101}\sin\theta = \lambda$.
[b] The value was calculated from $a = d_{101}\sqrt{2}$.
[c] The value was determined by BET method.
[d] The average pore diameter was estimated using the desorption curve of the isotherm and BJH model.
[e] The value was calculated from Tauc plot.
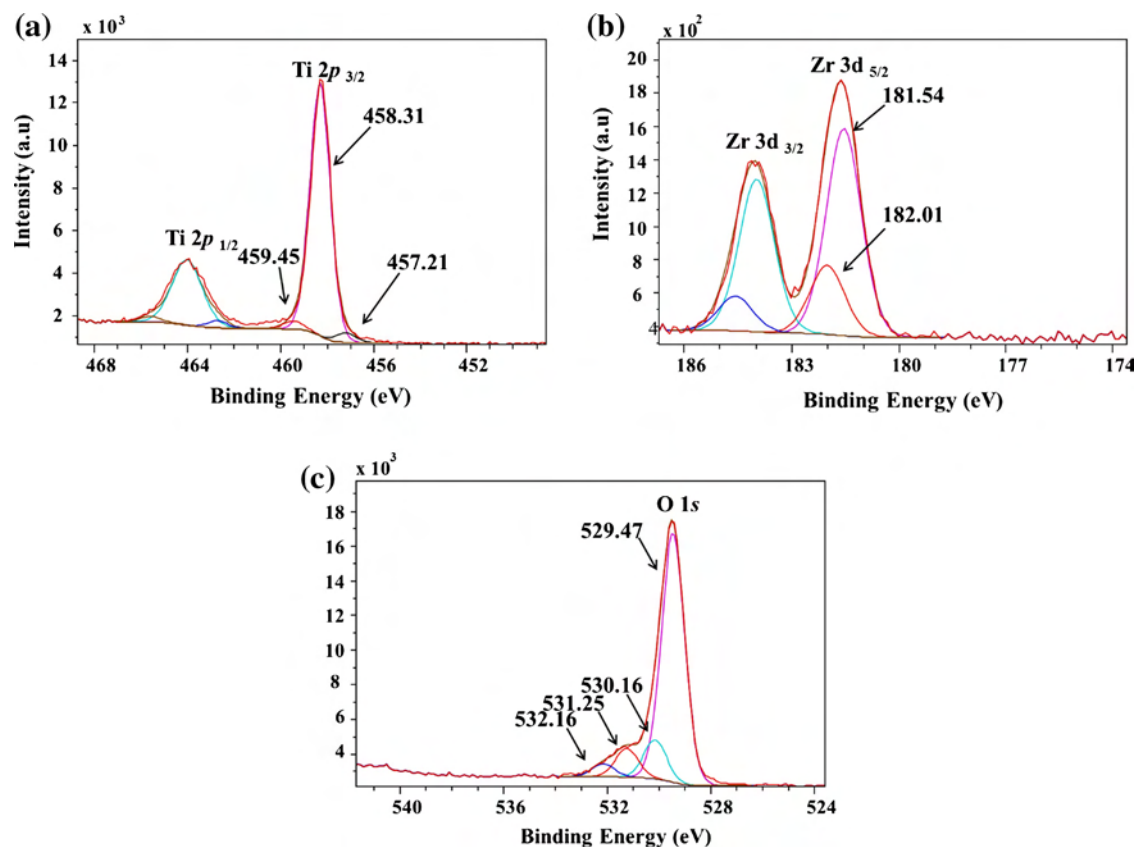
Figure 2 XPS spectra of ZrO₂/TiO₂ (20:80) photocatalyst (a) Ti 2p and (b) Zr 3d and O 1s.

The shifting in binding energy might be due to the electron transfer from Zr^{4+} to Ti^{4+} and formation of Ti–O–Zr species. Moreover, the binding energy of XPS O 1s composed of four signals at 529–532 eV corresponded to the lattice oxygen (Ti/Zr–O) and surface hydroxyl groups (Ti/Zr–OH) (Sun et al., 2011). The results obtained show that zirconium had undergone solid state reaction and forms ternary species and the remaining Zr was homogenously dispersed on TiO₂ surface or incorporated in TiO₂ lattice.

Fig. 3(a) shows the nanoparticles of ZrO₂/TiO₂ (20:80) photocatalyst were agglomerated with particle sizes ranging from 9 to 21 nm. HR-TEM image in Fig. 3(b) shows that the lattice fingers of anatase TiO₂ (1 0 1) were located close to ZrTiO₄ (1 1 1). Meanwhile, at upper part the rutile TiO₂ was detected near ZrTi₂O₆ that corresponding with (1 1 0) and (1 1 1) planes

respectively. This confirmed the existence of heterostructure in the catalyst interface that could retard the recombination of electron-hole.

Fig. 4 illustrates the N₂ adsorption–desorption isotherms of ZrO₂/TiO₂ photocatalysts that show adsorption of Type III at ratio of 10:90. Meanwhile, at ratio of 20:80 and 30:70 it shows the mixture of Type III and IV isotherms with the presence of mesoporous and macroporous materials and exhibited hysteresis loop of type H2(b) which associated with capillary condensation in ink bottle pores that have larger neck radius (Thommes et al., 2015). At the ratio of 10:90, the hysteresis loop was appeared at higher relative pressure indicating the weak interaction between adsorbate and adsorbent.

The largest specific surface area 46.35 m²/g was obtained at ratio 20:80 with average pore diameter of 177.21 Å which
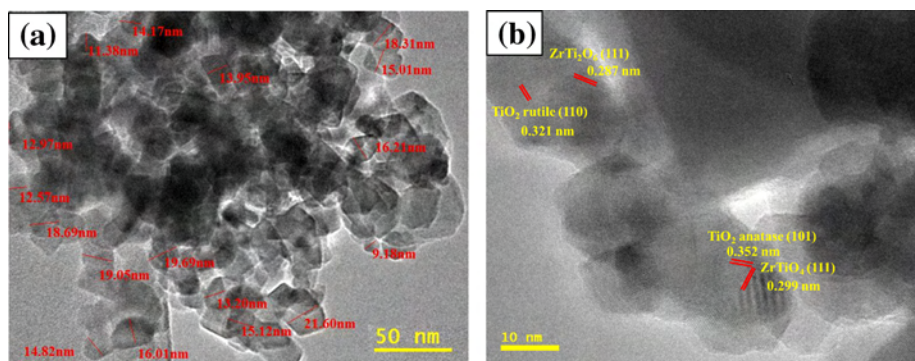
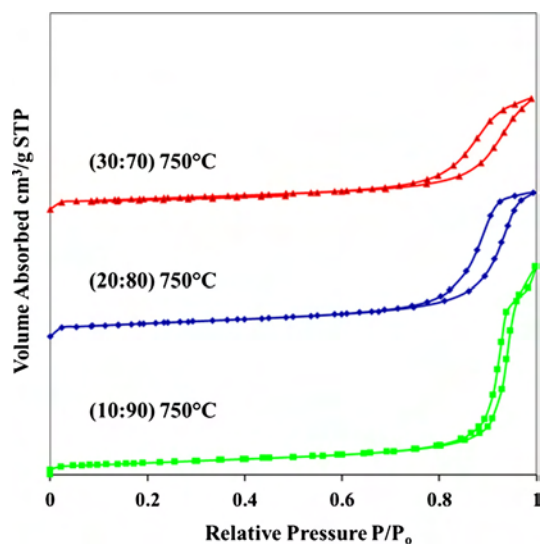**Figure 3**   (a) TEM and (b) HR-TEM images of ZrO$_2$/TiO$_2$ (20:80) photocatalyst calcined at 750 °C.

Figure 4   Isotherm plots of ZrO$_2$/TiO$_2$ photocatalysts at various ratios and were calcined at 750 °C for 5 h.

indicates higher adsorptibility compared to ratios 10:90 and 30:70 as listed in Table 3. At ratio 30:70 of ZrO$_2$/TiO$_2$, the ternary species were possibly deposited and covered the pore on the surface of photocatalyst leading to average pore diameter reduction and diminish the pore volume as proven by Wronski et al. (2015). This observation was supported by

XRD diffractogram (Fig. 1). ZrO$_2$/TiO$_2$ with ratio of 20:80 showed significant increment of catalyst surface area from ratio 10:90 due to more uniform particle distribution. It can be shown from the closing loop at P/P_o which was lower than the ratio of 10:90.

The optical properties were examined by using UV–Vis diffuse reflectance spectroscopy. Fig. 5 shows the band absorption edge was shifted to shorter wavelength when the Zr ratio was increased from 10:90 to 30:70. This might be due to the formation of ternary species as shown in XRD and XPS analyses. In contrast, Gao et al. (2010) stated that the formation of Ti$_2$ZrO$_6$ shifted the absorption band to longer wavelength at visible region with ratio 35:65.

Two absorption bands at 250 nm and 320 nm were observed indicating the presence of nano-sized of TiO$_2$ and assigned to ligand to metal charge transfer transition O$^{2-} \rightarrow$ Ti^{4+} (or Zr^{4+}) as also stated by Anzures et al. (2015) and Stefan et al. (2014). Besides that, overlapping at longer wavelength suggested the coexistence of heterojunction which is supported by the formation of hysteresis loop shown in Fig. 4. The extrapolated line fitted to the linear portions was carried out as shown in Fig. 5(b) to determine the band gap energy of the photocatalyst. Increasing of ZrO$_2$/TiO$_2$ ratio displayed bigger band gap energy might be due to the suppression of anatase to rutile phase transformation in the photocatalyst as shown in Table 3. Furthermore, it was concluded that the formation of heterojunction of ZrTiO$_4$/ZrTi$_2$O$_6$/TiO$_2$ has demonstrated larger band gap energy as illustrated from Tauc plot (Table 3).

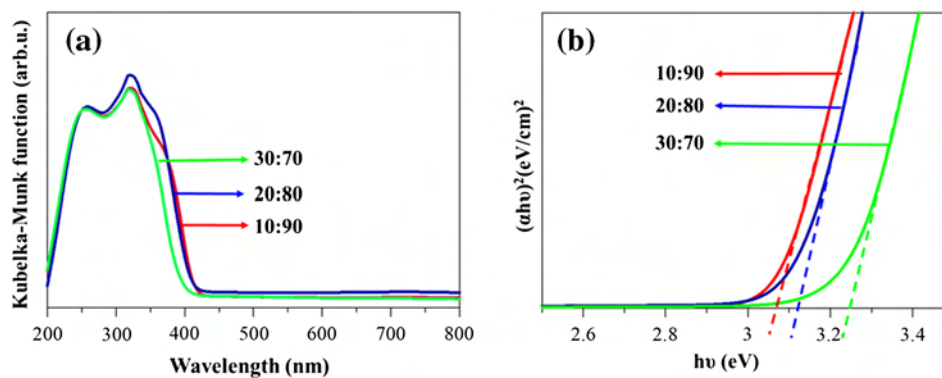**Figure 5**   (a) DR UV–Vis spectra and (b) Tauc plots of ZrO$_2$/TiO$_2$, with various ZrO$_2$/TiO$_2$ ratios calcined at 750 °C for 5 h.

3.2. Evaluation of photocatalytic activity

The control experiments were conducted to test the stability of paraquat dichloride before undergoing photodegradation reaction. Fig. 6 shows that 9.08% of paraquat dichloride was degraded without the presence of catalyst (photolysis), showing that paraquat dichloride is quite stable under UV irradiation (Cantavenera et al., 2007). Meanwhile adsorption/desorption experiment gave only 3.64% of paraquat dichloride degradation after 240 min reaction time. Interestingly, remarkable enhancement was obtained in the presence of UV irradiation and TiO$_2$ calcined at 450 °C as photocatalyst that gave 22.41% of paraquat dichloride degradation after 240 min irradiation.

Fig. 7 shows kinetic study of paraquat dichloride using ZrO$_2$/TiO$_2$ photocatalyst at various ZrO$_2$/TiO$_2$ ratios and TiO$_2$ calcined at 450 °C for comparison study. The linear plots of ln(C/C_o) versus irradiation time (t) that parallels to a pseudo first-order reaction kinetics analysis, which its usual form as shown in Eq. (3). The relevant data are tabulated in Table 4.

$$\ln(C/C_o) = -kt \tag{3}$$

where C is the paraquat concentration at t time, t is refer to reaction time (min), C_o is the initial concentration of paraquat and k is the rate constant of the change in the paraquat dichloride concentration (min^{-1}). The ZrO$_2$/TiO$_2$ at ratio of 20:80 demonstrated that at lower paraquat concentration and higher Zr ratio the kinetic study has deviated from pseudo first-order reaction kinetic as also reported by McMurray et al. (2006).
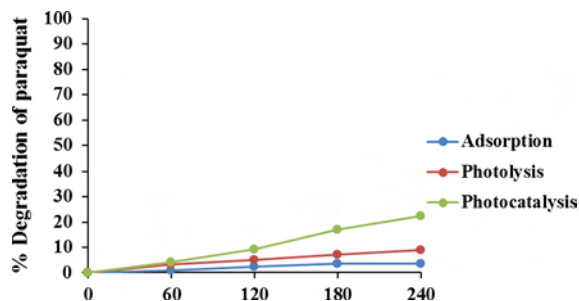
Table 4 Kinetic values for the photodegradation of paraquat dichloride under UV irradiation, $\lambda_{UV} = 365$ nm.

Photocatalyst	Rate constant, k (min^{-1})	R^2
TiO$_2$-450 °C	0.0011	0.99
10:90–750 °C	0.0054	0.99
[a]20:80–750 °C	0.0056	0.99
[a]30:70–750 °C	0.0037	0.99

[a] The values were measured in the range 0–180 min reaction time.

Figure 8 Photodegradation of paraquat dichloride over ZrO$_2$/TiO$_2$ (20:80) photocatalyst calcined at 750 °C for 5 h at various catalyst dosages. [paraquat] = 15 ppm, $\lambda_{UV} = 365$ nm and reaction time = 240 min.

Figure 6 Control experiment under different reaction systems, [paraquat, PQ] = 15 ppm, $\lambda_{UV} = 365$ nm, reaction time = 240 min. Catalysts = TiO$_2$ (450 °C, 0.1 g).
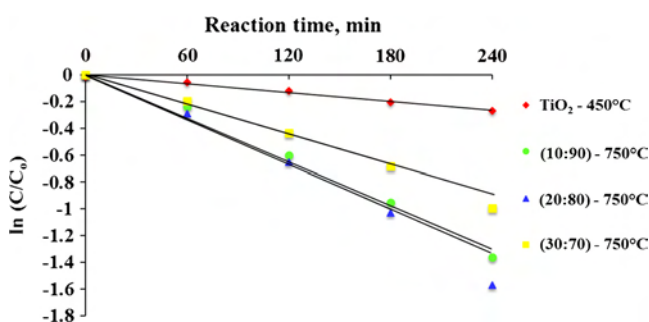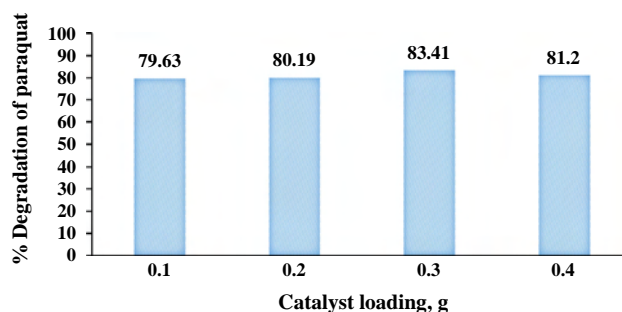

Figure 7 Pseudo first order kinetics of paraquat dichloride degradation.

Among the photocatalysts tested, ZrO$_2$/TiO$_2$ at ratio 20:80 showed highest degradation rate constants implying its higher degradability as compared to the TiO$_2$, ZrO$_2$/TiO$_2$ (10:90) and ZrO$_2$/TiO$_2$ (30:70) (Table 4). This verifies that the presence of ZrTiO$_4$/ZrTi$_2$O$_6$/TiO$_2$ and rutile phase of TiO$_2$ at ratio anatase to rutile 82:18 in the photocatalyst system led to the increase paraquat dichloride the photodegradation.

Further investigation was carried out using various catalyst dosages from 0.1 to 0.4 g of ZrO$_2$/TiO$_2$ (20:80) photocatalyst (Fig. 8) to gain the optimum photodegradation of paraquat dichloride. The order photocatalytic activity of 0.3 > 0.4 > 0.2 > 0.1 g was observed. From the results obtained, the optimum catalyst loading for ZrO$_2$/TiO$_2$ (20:80) was 0.3 g which gave 83.41% of paraquat dichloride degradation after 240 min reaction. Increasing the catalyst dosage increases the amount of active site and led to the increasing photodegradation of paraquat dichloride up to 0.3 g. In contrast, further increase of catalyst dosage up to 0.4 g lowers the photodegradation of paraquat dichloride. This might be due to scattering effect caused by increasing the turbidity of suspension that prevents UV light penetration into water as also observed by Bensaadi et al. (2014). In addition, Ahmed et al. (2011) had also reported that the agglomeration of catalyst might occur in the excess of catalyst dosage and this will result in the reduction of active site of the catalyst.

From the parameters studied, it can be summarized that the optimum condition for degradation of paraquat using ZrO$_2$/TiO$_2$ photocatalyst was obtained at calcination temperature of 750 °C with ZrO$_2$/TiO$_2$ ratio of 20:80 and 0.3 g of catalyst dosage which gave 8.41% degradation of paraquat dichloride after 240 min irradiation.

Table 5 ANOVA results of the quadratic model for photodegradation of paraquat dichloride.

Source	Sum of squares	Degree of freedom	Mean square	F-value	P-value
Model	3143.50	9	349.28	2083.24	<0.0001
A	348.61	1	348.61	2079.27	<0.0001
B	555.78	1	555.78	3314.90	<0.0001
C	9.97	1	9.97	59.45	0.0001
AB	111.72	1	111.72	666.37	<0.0001
AC	0.038	1	0.038	0.23	0.6484
BC	1.59	1	1.59	9.47	0.0179
A^2	1828.87	1	1828.87	10908.19	<0.0001
B^2	62.05	1	62.05	370.07	<0.0001
C^2	114.79	1	114.79	684.63	<0.0001
Residual	1.17	7	0.17		
Lack of fit	0.056	3	0.019	0.067	0.9745
Pure error	1.12	4	0.28		
Total	3144.68	16			

4. The optimization of Zr/Ti photocatalyst by Box–Behnken design

The Box–Behnken design was employed and 17 experiments were taken at random orders for optimization study. The variables are selected which were calcination temperature (A), ZrO$_2$/TiO$_2$ ratio (B) and catalyst dosage (C). The final quadratic equation was attained to elucidate the mathematical connection between the independent parameters and the dependent respond (Y) as presented in Eq. (4):

Photodegradation of paraquat dichloride (Y)

$$= 83.07 + 6.60A - 8.33B + 1.12C + 5.28AB$$
$$- 0.097AC + 0.63BC - 20.89A^2 - 3.89B^2 - 5.27C^2 \quad (4)$$

Table 5 shows the model is significant with the F-value is 2083.24 with corresponding p-value < 0.0001.

There is only a 0.01% chance that a larger "Model F-value" could occur due to noise. The lack of fit was not significant with F-value 0.067 and the p-value was 0.9745. In this study, the independent variable of the quadratic model calcination temperature (A), ZrO$_2$/TiO$_2$ ratio (B), catalyst dosage (C), the interaction between calcination temperature and ZrO$_2$/TiO$_2$ ratio and the interaction between ZrO$_2$/TiO$_2$ ratio and catalyst dosage are quite significant with the p-value less than 0.05. The ZrO$_2$/TiO$_2$ ratio was the most influent parameter which achieved 3314.90 F-value followed by calcination temperature (2079.27) and catalyst dosage (59.45). The high R^2 value of 0.9996 indicates that the quadratic model is fitted with the data. The predicted R^2 value of 0.9992 is in reasonable agreement with the adjusted R^2 value of 0.9991. Fig. 9 shows a comparison between predicted and actual values of the response and confirms that the results obtained are in a good agreement with the predicted values.

Three dimensional response surfaces of photodegradation of paraquat dichloride as function of (a) calcination versus ZrO$_2$/TiO$_2$ ratio (catalyst dosage = 0.3 g), (b) calcination temperature versus catalyst dosage (ZrO$_2$/TiO$_2$ ratio = 20) and (c) ZrO$_2$/TiO$_2$ ratio versus catalyst dosage (calcination temperature = 750 °C) are presented in Fig. 10.

The coordinates of central point within the maximum contour levels represent the optimal values of the respective
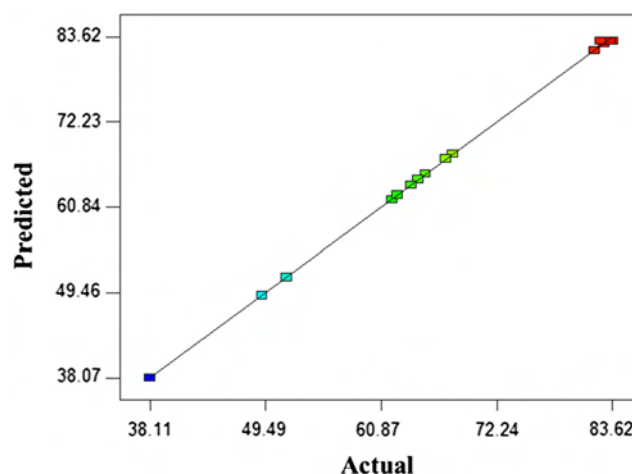

Figure 9 The relationship of predicted and actual values for BBD.

parameters. Fig. 10(a) and (b) shows that calcination temperature gave significant enhancement on the photodegradation of paraquat dichloride until achieving the optimum point. The higher photodegradation of paraquat dichloride was obtained at higher catalyst dosage with lower ZrO$_2$/TiO$_2$ ratio as shown in Fig. 10(c). This might be due to the phase transformation of anatase to rutile and the formation of heterojunction of ZrTiO$_4$/ZrTi$_2$O$_6$/TiO$_2$ as shown in Figs. 1 and 2 as also reported by Gnatyuk et al. (2010).

To achieve the optimum condition for this model, each variable was adjusted to attain the maximum photodegradation of paraquat dichloride. The optimum condition for this model was achieved at calcination temperature 750 °C, 20% ZrO$_2$/TiO$_2$ ratio and 0.3 g catalyst dosage with 83.65% degradation of paraquat dichloride. An additional experimental was carried out under the optimum condition to confirm the agreement of the model and experimental data. The experimental value obtained was 83.17% which is in good agreement with the predicted results thus validated the finding of response surface optimization with percentage error of 0.24%.
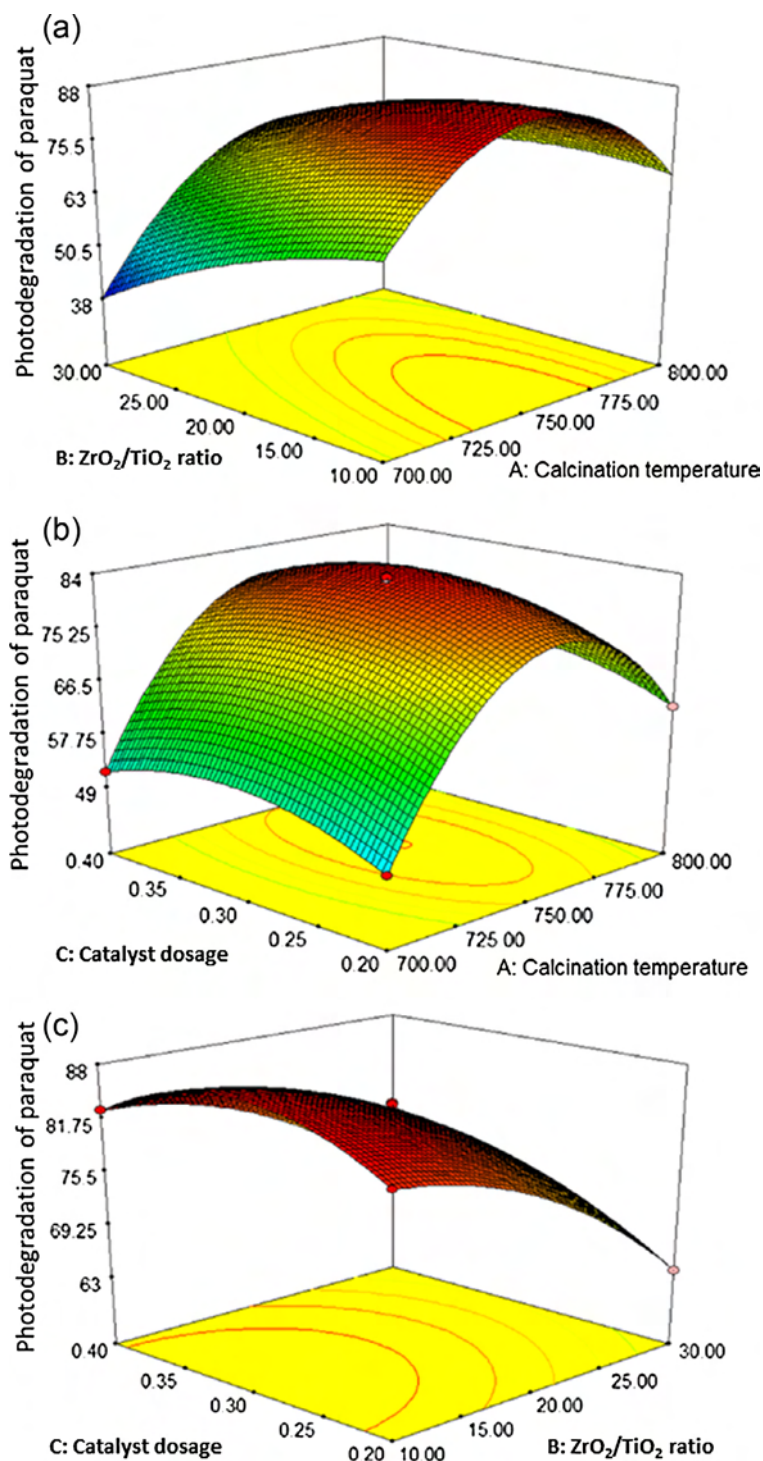
Figure 10 3-D surface plots of photodegradation as a function of (a) calcination temperature and ZrO_2/TiO_2 ratio, (b) calcination temperature and catalyst dosage and (c) ZrO_2/TiO_2 ratio and catalyst dosage.

5. Conclusion

The ZrO_2/TiO_2 photocatalyst was successfully synthesized using modified sol gel method. The existence of heterojunction of $TiZrO_4/Ti_2$-ZrO_6/TiO_2 photocatalyst was confirmed using XRD and XPS analyses and was acted as anatase phase stabilizer and gave remarkable enhancement for the photodegradation of paraquat dichloride.

Optimum photodegradation of paraquat dichloride was obtained using ZrO_2/TiO_2 atomic ratio of 20:80 calcined at 750 °C for 5 h with 0.3 g of catalyst dosage. This reaction followed the pseudo first order kinetic equation. The Box–Behnken experimental design revealed that the optimum photodegradation of paraquat was achieved at 750 °C, with Zr ratio (20:80) and 0.3 g catalyst dosage that gave 83.41% degradation which is 0.24% different from the experimental result.

Acknowledgments

References

Ahmed, S., Rasul, M.G., Brown, R., Hashib, M.A., 2011. J. Environ. Manage. 92, 311–330.

Ali, R., Hassan, S.H., 2008. Malaysian J. Anal. Sci. 12, 77–87.

Anzures, F.M., Rivas, F.C., Ventura, J.H., Hernández, P.S., Berlier, G., Zacahua-Tlacuatl, G., 2015. Appl. Catal. A Gen. 489, 218–225.

Badli, N.A., Ali, R., Yuliati, L., 2015. Adv. Mater. Res. 1107, 377–382.

Bensaadi, Z., Yeddou-Mezenner, N., Trari, M., Medjene, F., 2014. J. Environ. Chem. Eng. 2, 1371–1377.

Cantavenera, M.J., Catanzaro, I., Loddo, V., Palmisano, L., Sciandrello, G., 2007. J. Photochem. Photobiol. A Chem. 185, 277–282.

Dhaouadi, A., Adhoum, N., 2009. J. Electroanal. Chem. 637, 33–42.

Florêncio, M.H., Pires, E., Castro, A.L., Nunes, M.R., Borges, C., Costa, F.M., 2004. Chemosphere 55, 345–355.

Gao, B., Lim, T.-T.T.M., Subagio, D.P., Lim, T.-T.T.M., 2010. Appl. Catal. A Gen. 375, 107–115.

Gnatyuk, Y., Smirnova, N., Korduban, O., Eremenko, a., 2010. Surf. Interf. Anal. 42, 1276–1280.

Kim, C.-S., Shin, J.-W., An, S.-H., Jang, H.-D., Kim, T.-O., 2012. Chem. Eng. J. 204–206, 40–47.

Kim, S.W., Khan, R., Kim, T., Kim, W., 2008. Bull. Korean Chem. 29, 1217–1223.

Lee, J.-C., Kim, M.-S., Kim, B.-W., 2002. Water Res. 36, 1776–1782.

Madani, M.El., Harir, M., Zrineh, A., Azzouzi, M.El., 2015. J. Chem. 8, 181–185.

McMurray, T.A., Dunlop, P.S.M., Byrne, J.A., 2006. J. Photochem. Photobiol. A Chem. 182, 43–51.

Santos, M.S.F., Alves, A., Madeira, L.M., 2011. Chem. Eng. J. 175, 279–290.

Schiller, R., Weiss, C.K., Landfester, K., 2010. Nanotechnology 21, 405–603.

Sorolla, M.G., Dalida, M.L., Khemthong, P., Grisdanurak, N., 2012. J. Environ. Sci. 24, 1125–1132.

Stefan, M., Pana, O., Leostean, C., Bele, C., Silipas, D., Senila, M., Gautron, E., 2014. J. Appl. Phys. 116, 114312-1–114312-11.

Sun, C., Liu, L., Qi, L., Li, H., Zhang, H., Li, C., Gao, F., Dong, L., 2011. J. Colloid Interf. Sci. 364, 288–297.

Thommes, M., Kaneko, K., Neimark, A.V., Olivier, J.P., Rodriguez-Reinoso, F., Rouquerol, J., Sing, K.S.W., 2015. Pure Appl. Chem., 1051–1069

Venkatachalam, N., Palanichamy, M., Arabindoo, B., Murugesan, V., 2007. J. Mol. Catal. A Chem. 266, 158–165.

Wronski, P., Surmacki, J., Abramczyk, H., Adamus, A., Nowosielska, M., Maniukiewicz, W., Kozanecki, M., Szadkowska-Nicze, M., 2015. Radiat. Phys. Chem. 109, 40–47.